Supporting Information

Supplementary figures

Figure S1

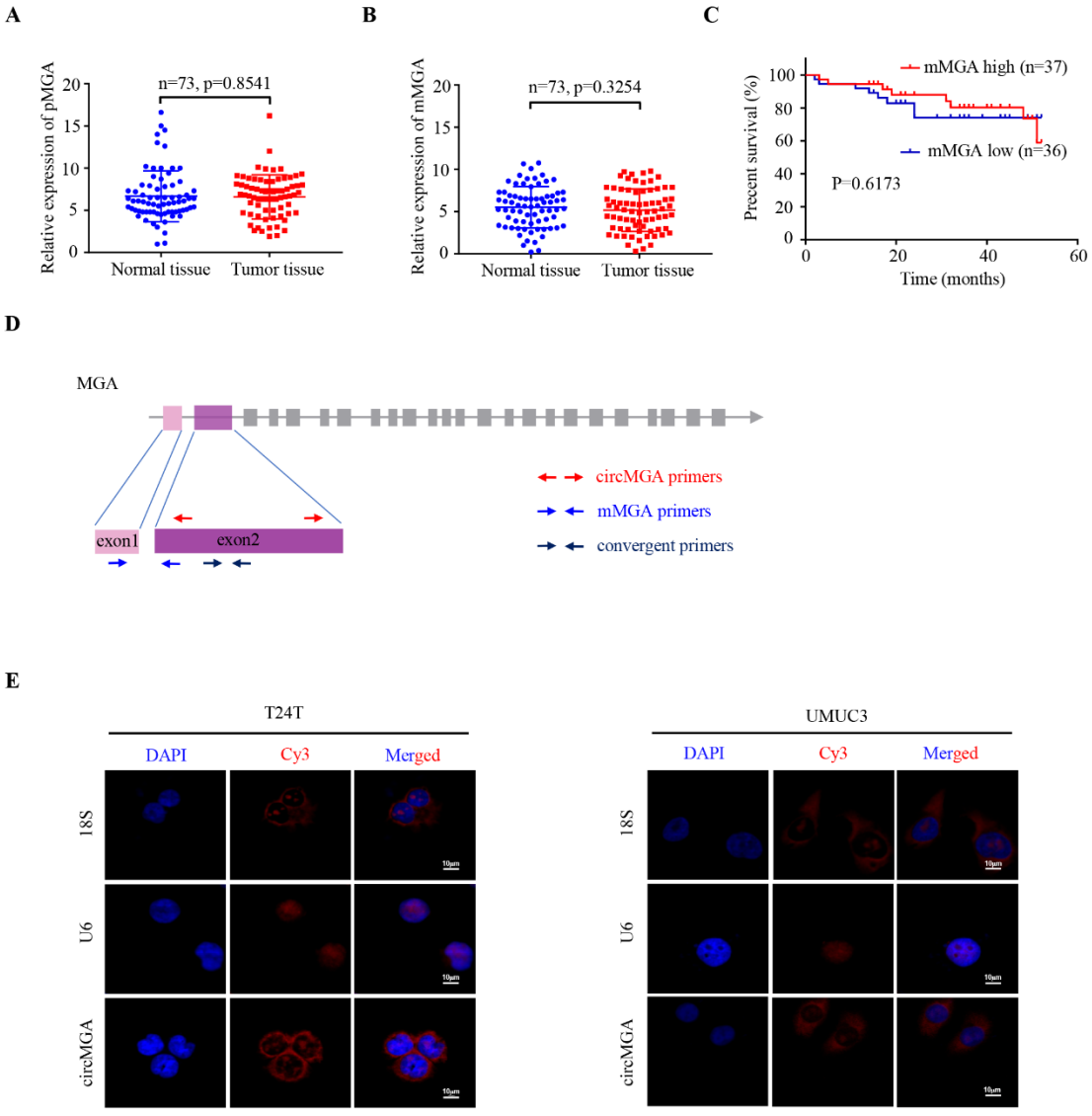

Figure S1: CircMGA mainly distributes in the cytoplasm of bladder cancer cells. **A.** and **B.** The expression of MGA pre-mRNA (pMGA) and mRNA (mMGA) were detected by qRT-PCR in 73 pairs of bladder cancer and paired adjacent normal bladder tissues, respectively. GAPDH was used as internal control. Data were mean ± SD, paired t-test. **C.** Kaplan-Meier curves of

OS in bladder cancer patients. Patients were grouped by the median mMGA expression. *P*-value was calculated using a log-rank test. **D.** Schema for the primers. **E.** Identification of circMGA cytoplasmic and nuclear distribution by FISH in T24T (left) and UMUC3 (right) cells. 18S and U6 were used as positive controls in the cytoplasm and nucleus, respectively. circMGA, 18S and U6 probes were labeled with Cy3, Nuclei were stained with DAPI. Scale bar, 10 μm.

Figure S2

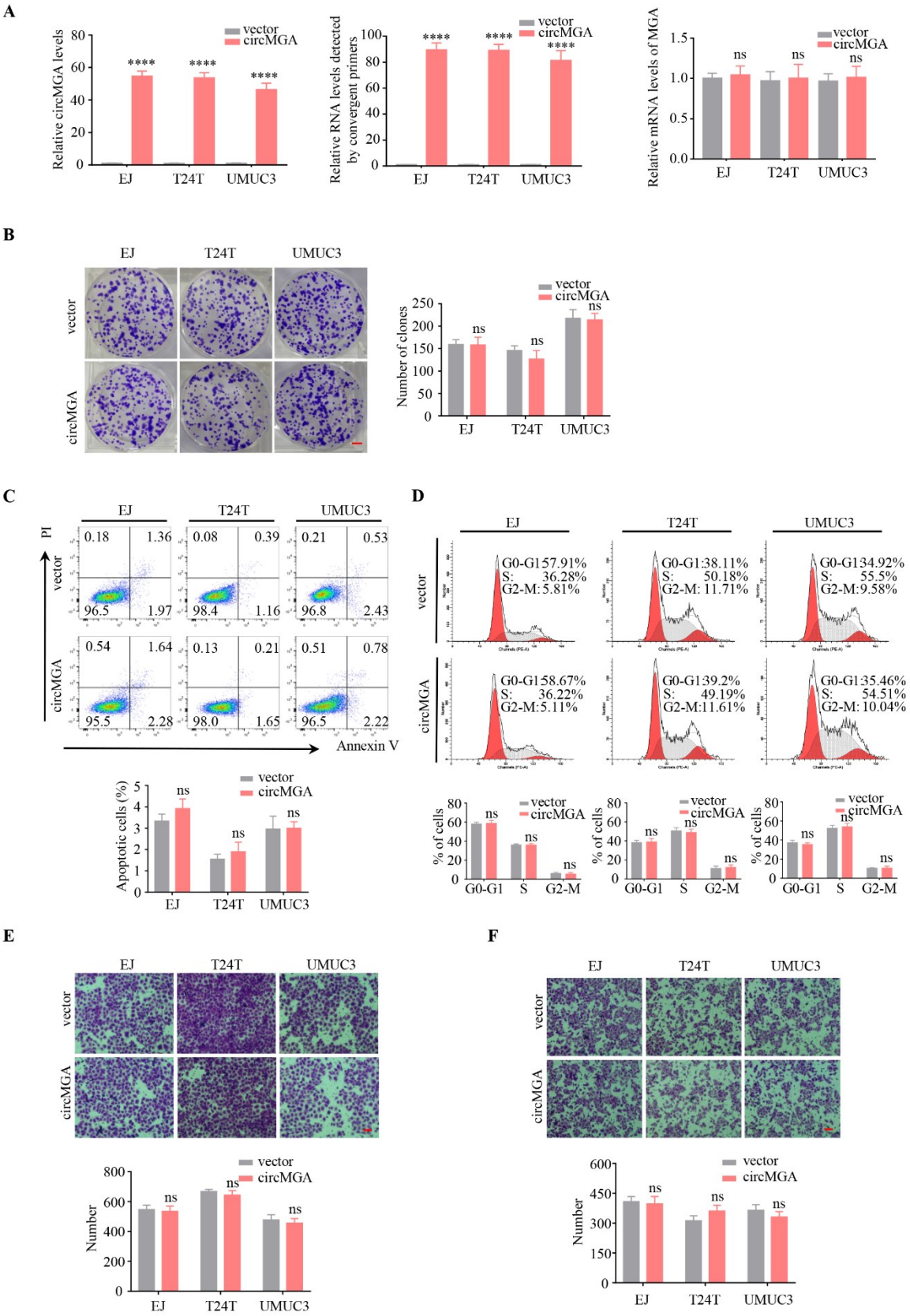
A
Relative circMGA levels
vector
circMGA
****
EJ
T24T
UMUC3
Relative RNA levels detected by convergent primers
Relative mRNA levels of MGA
ns
B
vector
circMGA
Number of clones
C
PI
Annexin V
0.18
1.36
96.5
1.97
0.08
0.39
98.4
1.16
0.21
0.53
96.8
2.43
0.54
1.64
95.5
2.28
0.13
0.21
98.0
1.65
0.51
0.78
96.5
2.22
Apoptotic cells (%)
D
G0-G1 57.91%
S: 36.28%
G2-M: 5.81%
G0-G1 38.11%
S: 50.18%
G2-M: 11.71%
G0-G1 34.92%
S: 55.5%
G2-M: 9.58%
G0-G1 58.67%
S: 36.22%
G2-M: 5.11%
G0-G1 39.2%
S: 49.19%
G2-M: 11.61%
G0-G1 35.46%
S: 54.51%
G2-M: 10.04%
% of cells
G0-G1
S
G2-M
E
Number
F
Number

Figure S2: CircMGA does not affect cell viability and metastasis. **A.** QRT-PCR was used to detect the expression levels of circMGA (left), linear isoform transcribed from circMGA (middle) or mRNA of MGA (right) in EJ, T24T and UMUC3 cells treated with stably overexpressing circMGA or vector. **B.** The cell proliferative ability was detected by colony formation assay with stably overexpressing circMGA in EJ, T24T and UMUC3 cells. **C.** The apoptosis ratio of bladder cancer cells was determined. **D.** Cell cycle analysis of bladder cancer cells with stably overexpressing circMGA or vector. **E.** Cell migration abilities of EJ, T24T and UMUC3 cells transfected with circMGA or vector were detected by transwell migration assay. Data were mean ± SD, n = 3. Scale bar, 100 μm. **F.** Cell invasion abilities of EJ, T24T and UMUC3 cells transfected with circMGA or vector were detected by transwell matrigel invasion assay. Data were mean ± SD, n = 3. Scale bar, 100 μm. Data information: In (A-D), data are presented as mean ± SD. ns means no statistical significance, ****$P< 0.0001$ (Student's t-test).

Figure S3

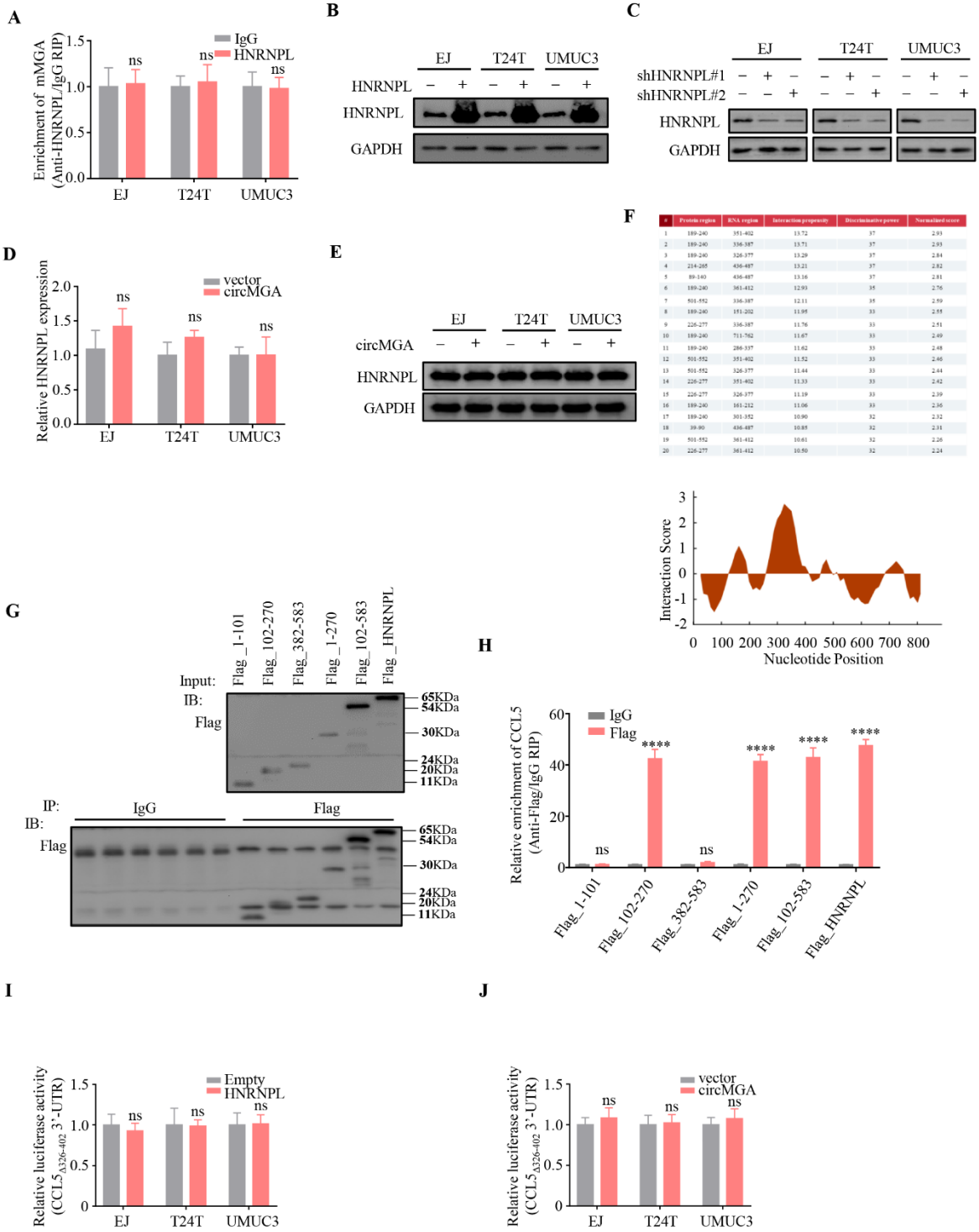
A
Enrichment of mMGA (Anti-HNRNPL/IgG RIP)
IgG
HNRNPL
ns
EJ
T24T
UMUC3
B
EJ
T24T
UMUC3
HNRNPL
GAPDH
C
shHNRNPL#1
shHNRNPL#2
D
Relative HNRNPL expression
vector
circMGA
E
circMGA
F
Interaction Score
Nucleotide Position
G
Input:
IB:
Flag
Flag_1-101
Flag_102-270
Flag_382-583
Flag_1-270
Flag_102-583
Flag_HNRNPL
65KDa
54KDa
30KDa
24KDa
20KDa
11KDa
IP:
IgG
H
Relative enrichment of CCL5 (Anti-Flag/IgG RIP)
****
I
Relative luciferase activity (CCL5Δ326-402 3'-UTR)
Empty
J

Figure S3: HNRNPL bind with CCL5 mRNA in bladder cancer cells. **A.** RIP assays showed the relationship between HNRNPL and mMGA. The HNRNPL-enriched mMGA relative to the IgG-enriched value was calculated by qRT-PCR, IgG antibody used as a control. **B.** and **C.** The expression levels of HNRNPL in bladder cancer cells were detected by western blot. **D.** The mRNA levels of HNRNPL in bladder cancer cells with or without overexpression of circMGA were determined by qRT-PCR. **E.** Western blot analysis with the indicated antibodies in bladder cancer cells stably transfected with vector or circMGA. **F.** CatRAPID algorithm was used to predict the RNA-protein interaction of CCL5 mRNA 3'-UTR with HNRNPL. **G.** Immunoblot analysis with anti-Flag of T24T cells transfected with plasmids encoding Flag-tagged HNRNPL or truncated HNRNPLs. **H.** Relative enrichment of CCL5 in full-length or truncated HNRNPL RIP was measured by qRT-PCR. **I.** Dual-luciferase assay revealing the relative luciferase activities of $CCL5_{\triangle 326\text{-}402}$ 3'-UTR in bladder cancer cells stably transfected with or without HNRNPL. **J.** Dual-luciferase assay revealing the relative luciferase activities of $CCL5_{\triangle 326\text{-}402}$ 3'-UTR in bladder cancer cells stably transfected with or without circMGA. Data information: In (A, D and H-J), data are presented as mean ± SD. ns means no statistical significance, ****$P<$ 0.0001 (Student's t-test).

Figure S4

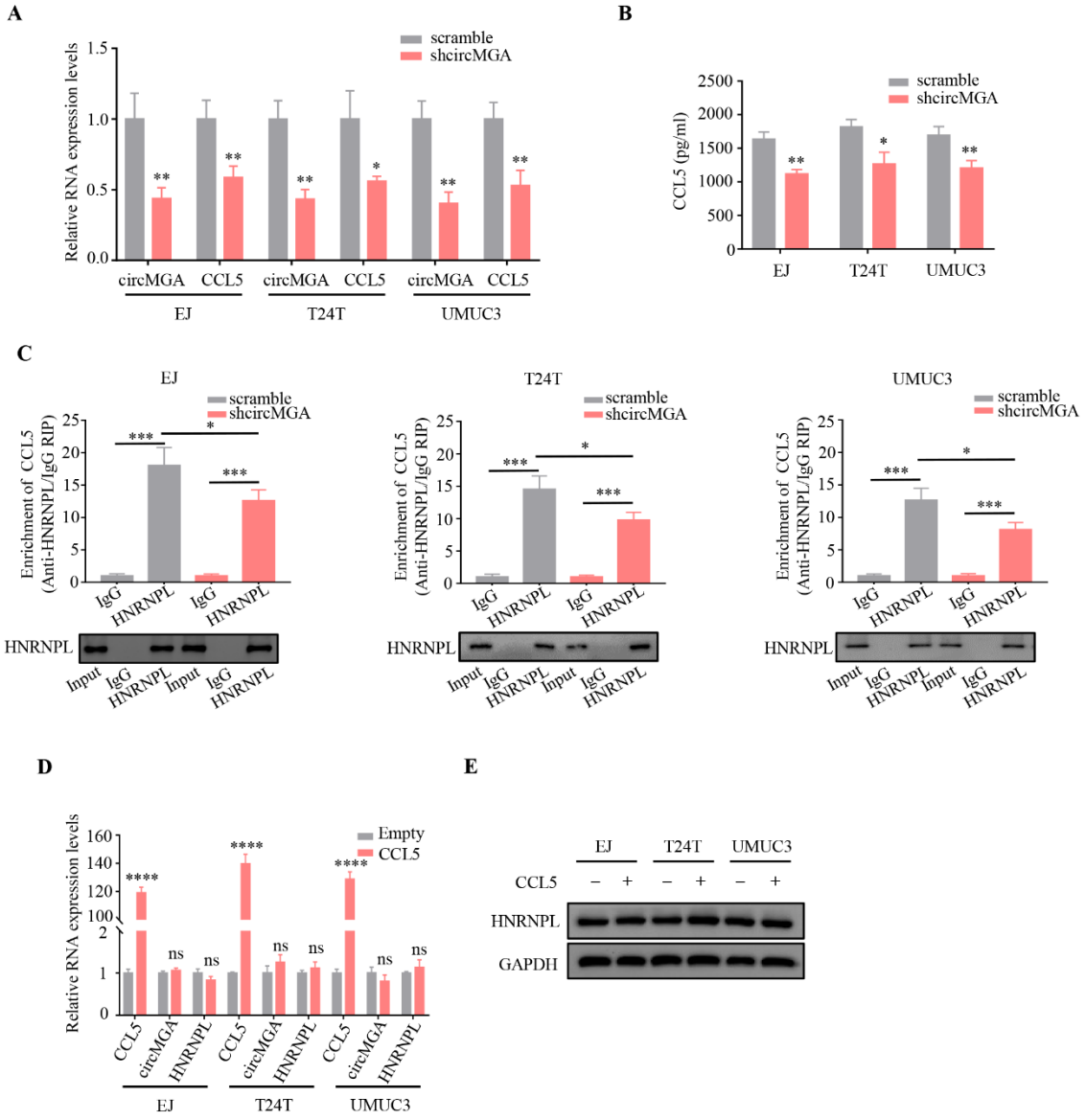

Figure S4: Knockdown of circMGA decreases the accumulation of CCL5. **A.** The RNA levels in bladder cancer cells with or without knockdown of circMGA were determined by qRT-PCR. **B.** The expression and secretion of CCL5 in bladder cancer cells with or without knockdown of circMGA were detected by ELISA. **C.** Relative enrichment of endogenous CCL5 mRNA in RIP analysis, following bladder cancer cells transfected with or without knockdown of circMGA. Top, The HNRNPL-enriched CCL5 relative to the IgG-enriched value was calculated by qRT-PCR. Bottom, IP efficiency of HNRNPL antibody shown in western blotting. IgG antibody used as a control. **D.** The mRNA levels in bladder cancer cells stably transfected

with empty or CCL5 were determined by qRT-PCR. **E.** The expression levels of HNRNPL in bladder cancer cells with or without overexpression of CCL5 were detected by western blot. Data information: In (A-D), data are presented as mean ± SD. ns means no statistical significance, *P< 0.05, **P< 0.01, ***P< 0.001,****P< 0.0001 (Student's t-test).

Figure S5

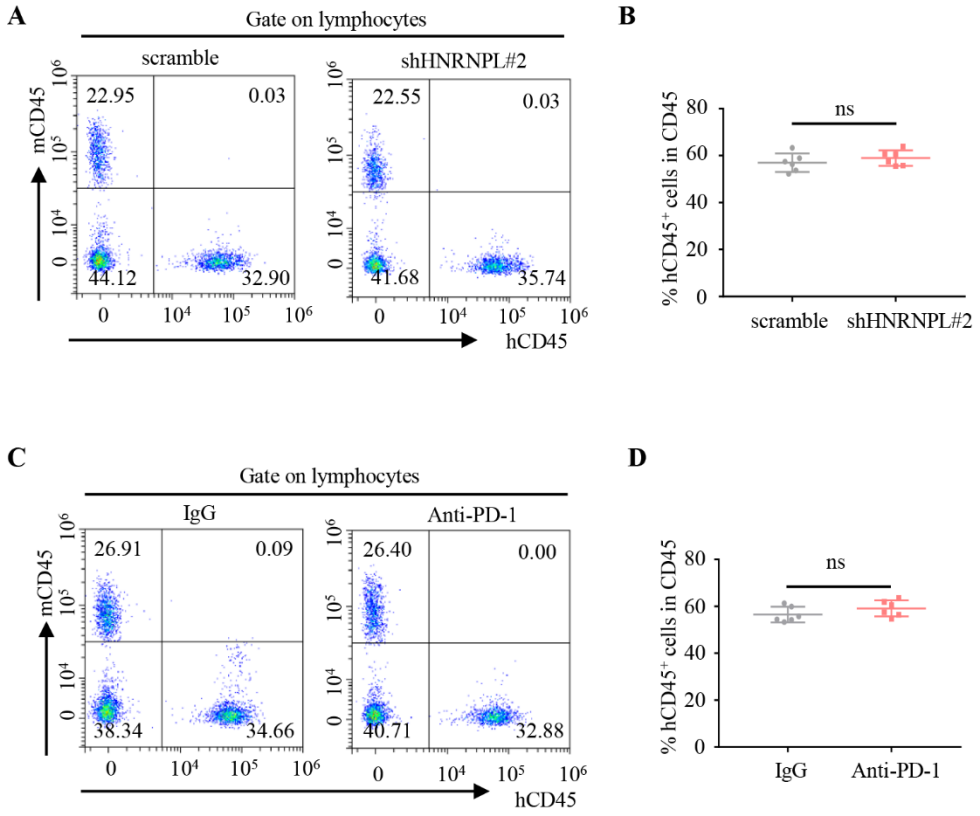

Figure S5: Establishment of Hu-HSC-NPG mice. **A.** Representative FCM profiles of human CD45$^+$ (hCD45$^+$) cells and mouse CD45$^+$ (mCD45$^+$) cells in circulating blood of reconstituted Hu-HSC-NPG mice bearing subcutaneous xenograft tumors of EJ cells transfected accordingly. Plots were gated on lymphocytes. **B.** Repopulation of hCD45$^+$ cells among CD45$^+$ (hCD45$^+$ and mCD45$^+$) lymphocytes in circulating blood of reconstituted Hu-HSC-NPG mice in (A). Each point in the scatter plot represents blood drawn from an individual mouse (n = 6). **C.** Representative FCM profiles of hCD45$^+$ cells and mCD45$^+$ cells in circulating blood of reconstituted Hu-HSC-NPG mice bearing subcutaneous xenograft tumors of EJ cells with treatment accordingly. Plots were gated on lymphocytes. **D.** Repopulation of hCD45$^+$ cells among CD45$^+$ (hCD45$^+$ and mCD45$^+$) lymphocytes in circulating blood of reconstituted Hu-HSC-NPG mice in (C). Each point in the scatter plot represents blood drawn from an individual mouse (n = 6).

Supplementary dataset

Supplementary Table S1: Clinicopathological features and the expression of circMGA of 73 bladder cancer patients.

Supplementary Table S2: Sequences of primers, shRNAs and RNA pull down probes used in this study.

Supplementary Table S3: Mass spectrometry analysis of RNA pulldown.